CHAPTER II

Description & History of PTER

2.1 Physical Design

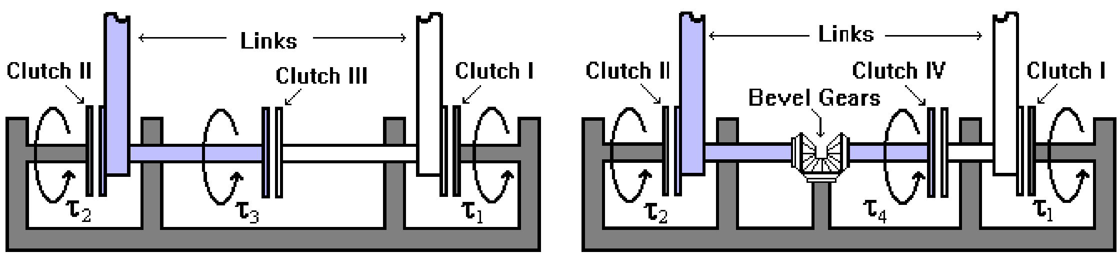

Figure 2.1: Clutch Configuration of PTER

PTER was designed and built by Robert Andrew Charles circa 1994. As stated before, the 2 DOF kinematics of PTER are based on the design of HURBIRT. Instead of using electric motors, Charles utilized four electromagnetic friction clutches; specifically Dynacorp Model 310 brakes. Because the Dynacorp clutches came with a small undesirable metal to metal contact area in addition to the friction pad interface, they were slightly modified to eliminate this adverse characteristic. Clutch locations can be seen in Figure 1.2, but illustrations of each clutch's operation can be viewed in Figure 2.1. In short, clutches 1 & 2 connect links 1 & 2 (respectively) to ground, while clutch 3 couples link 1 directly to link 2 and clutch 4 inversely couples the links. It can be seen that with only 2 DOF and four actuators, PTER is over actuated. This is a result of designing PTER to overcome some inherent limitations of using clutches as actuators. This will be revisited in a later section.

To measure user's input, a force sensor is incorporated in the handle of PTER. This force sensor takes advantage of Hook's law by using two sets of strain gauges to measure strain in the machined steel handle. The sensor is designed for compliance in two orthogonal directions, allowing full measurement of the 2-D input. Positioning of links 1 & 2 are measured through use of two 0-2KΩ / 360^{o} potentiometers. The majority of PTER is fabricated from aluminum, while the shafts and several miscellaneous components are steal.

2.2 Hardware

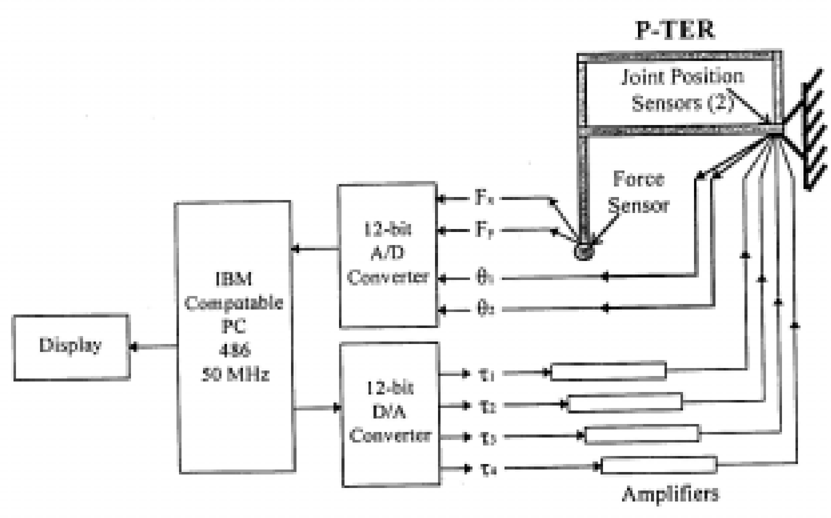

Figure 2.2: Hardware Illustration of PTER [Gomes, 1997]

PTER's intelligence came from a 486-50 MHZ IBM clone PC running DOS 6.21 and Windows for Workgroups 3.11. Programming by past students was performed using Borland C++ and real time interrupts were achieved by modifying DOS's original timer interrupt subroutine. Interface with the external hardware is through a Kiethley Metrabyte DAS-16 and a DDA-06. Two of the clutches are powered by a Kepco BOP 36-1.5 amplifier, another one by a Kepco Bop 36-5, while the final clutch is powered by a Kepco ATE 36-3. All of the amplifiers were operating in voltage mode, resulting in a relationship between amplifier output voltage and input voltage signal from the PC. Two Analog 3B18 strain gauge conditioners amplify and low-pass filter the strain gauge signals (@8.4 Hz) from the force sensor. A schematic of the system can be seen in Figure 2.2.

2.3 Impedance Control

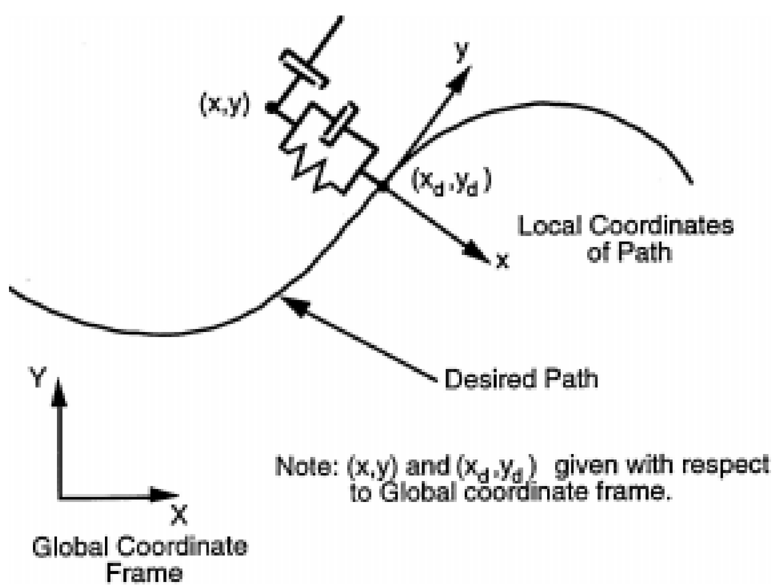

Figure 2.3: Impedance Control [Charles, 1994]

As stated earlier, the premise behind impedance control is to force the haptic device to behave like a targeted dynamic system. This can be more clearly explained using the desired path illustrated in figure 2.3. In this example the spring and damper shown, as well as a mass that is not shown, make up the target system. If the operator could perfectly guide the tip along the desired path, they would perceive that they were pushing a mass with a damper (the components tangent to the path). More realistically, if the operator pushed the device off the path, they would feel as if they were deflecting a mass – spring - damper system perpendicular to the path. This control strategy allows the programmer to simulate a wide variety of haptic features. Though a 2nd order linear system was used to illustrate the principle, the algorithm is by no means limited to linear targeted systems. To illustrate how this is implemented lets first define the following:

$J(\Theta)$	Haptic Interface's Jacobian relating joint velocities to global Cartesian velocities.
$J(\Theta)^T$	Jacobian's transpose relating Cartesian global input forces to joint forces / torques.
F_{in}	User input force in local Cartesian coordinates.
$R(\Theta)$	Rotation Matrix transforming local path Cartesian coordinates to global Cartesian coordinates
τ	Actuator's force / torque
$F(\ddot{X}, \dot{X}, X, t)$	Targeted dynamic system; ($F = M\ddot{X} + C\dot{X} + KX$) for the above 2nd order system.

Both the user's input force and the actuators affect the Haptic Interface’s dynamics. Therefore the following can be assumed as the interface’s generic dynamic equations of motion:

$$I(\Theta)\ddot{\Theta} + C(\Theta,\dot{\Theta})\dot{\Theta} + V(\Theta) = \tau + J(\Theta)^T R(\Theta) F_{in} \qquad \textbf{(2.1)}$$

By definition we wish to simulate our targeted dynamic system such that:

$$F(\ddot{X}, \dot{X}, X, t) = F_{in} \qquad \textbf{(2.2)}$$

Manipulating the dynamic equations for the Haptic Interface will result in:

$$[J(\Theta)^T R(\Theta)]^{-1}[I(\Theta)\ddot{\Theta} + C(\Theta,\dot{\Theta})\dot{\Theta} + V(\Theta) - \tau] = F_{in} \qquad \textbf{(2.3)}$$

Therefore, equating the two expressions we see the required actuator force / torque to achieve the simulated dynamic system is:

$$\tau = [I(\Theta)\ddot{\Theta} + C(\Theta,\dot{\Theta})\dot{\Theta} + V(\Theta)] - J(\Theta)^T R(\Theta) F(\ddot{X}, \dot{X}, X, t) \qquad \textbf{(2.4)}$$

Other approaches for determining actuator inputs given a targeted dynamic system have been implemented by past students, but the basic principle is the same; use of non-linear feedback to cancel the dynamics of the Haptic Interface and simulate a desired virtual boundary.

2.4 Implementation on PTER

The impedance control law was originally formulated for active haptic displays where any desired torque can be achieved as long as it is within the saturation limits of the actuator. The use of clutches in PTER resulted in a new set of restrictions. Clutches are dampers by nature and can only resist motion, but can not store energy or impart forces on a system at rest. One exception is when the system is at rest and the user is imparting a force. In this case clutches can only provide resistance equal and opposite to the users input, up until the point where motion begins. This has been a primary topic for past students working with PTER and why it was built over actuated. The required torques on the joints may not be realizable because of the direction of the users input force and systems velocity. In addition, to complicate matters, the solution to which actuators to use for the required torque may have infinite solutions.

2.4.1 Robert Andrew Charles

Robert Andrew Charles first attempted to address this problem and implement his solution on a simulation of PTER. [Charles, 1994] He determined an initial graphical and mathematical methodology for determining which combination of clutches to pick. Charles began by creating a 2-D plot with torque for brake one corresponding to the x-axis and torque for brake 2 corresponding to the y-axis. (See figure 2.4) He then plotted horizontal lines for brake 1's torque limits and vertical lines for brake 2's limits. This effectively sectioned off the space into regions of achievable torque from brakes one and two. Similarly, using equations based on PTER's configuration and the desired torque required for impedance control, Charles mapped limit lines for the inverting and direct coupling clutches with respect to required torque from brakes one and two. By looking at the overlapping regions, Charles could decide on what combinations of clutch actuation would result in the desired torque. He could also determine if no solution existed by the nonexistence of a region overlapped by all four limiting regions. Charles was only able to test his algorithm with a simulation of PTER and did not implement it on the actual test bed.

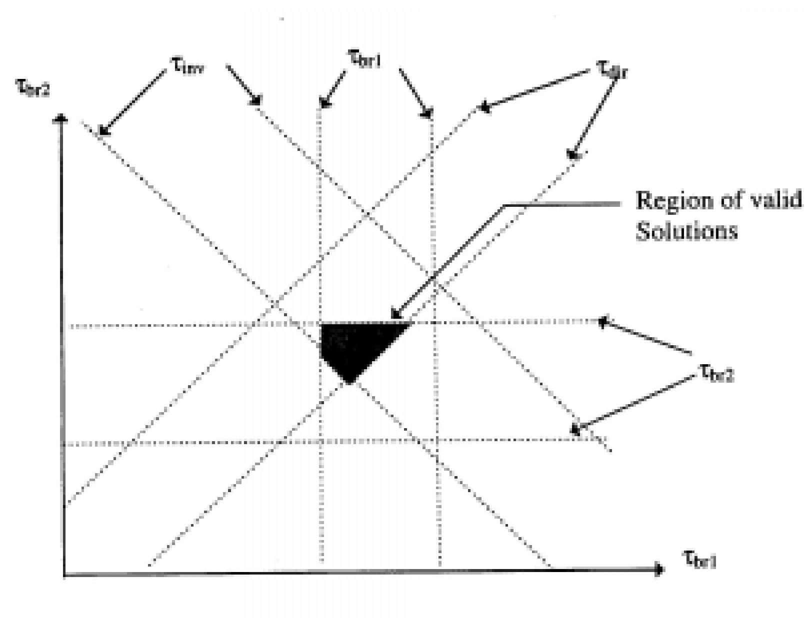

Figure 2.4: Charles's Mapping of Actuator Torque Limits [Charles, 1994]

2.4.2 Hurley Thomas Davis, Jr

Davis attempted to graphically characterize the available torque from each actuator as a function of current joint velocities. [Davis, 1996] Sixteen different cases are identified and mapped in joint velocity space. The direction, or unit vectors, of available torque from each actuator in a given case are graphically plotted in joint space. (See figure 2.5 for an example case) By comparing these unit vectors with desired torque for impedance control, one can intuitively see what linear combinations of actuators to use. It can also be seen that if the desired torque lies in a region not spanned by available actuators' torque, then the desired torque is not achievable. It should be noted that the clutches can not be negatively actuated, therefore unlike linear vector addition only positive combinations of actuator unit torque vectors can be used.

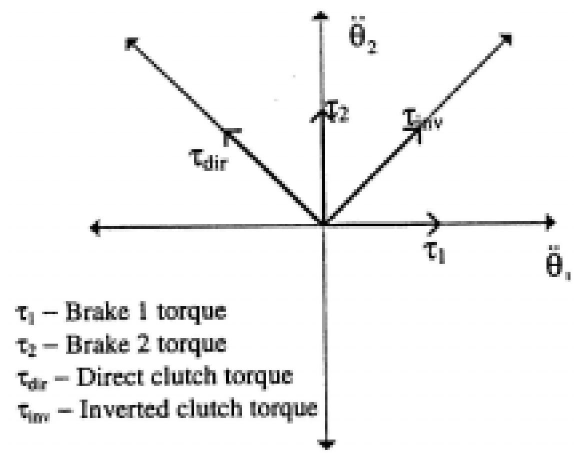

Figure 2.5: Plot of Available Torque for Davis's Case 12 [Davis, 1996]

Davis's algorithm uses only two clutches at one time and does not use any clutch whose relative angular velocity of the friction surfaces are zero. Davis also addresses the situation of an unachievable desired torque by choosing the combination of clutches that can achieve at least one component (in joint space) of the desired torque. This new algorithm was the first to be both simulated and tested on PTER. At that time, PTER's haptic algorithms were applied to trajectory following of a circle. Davis also investigated various values for stiffness of the target system. It was found that the algorithm was capable of tracking the general shape of the desired circle, but the operator experienced jerky movement of PTER's handle. Furthermore, actuator dynamic limitations began to surface.

2.4.3 Mario Waldorff Gomes

Gomes began by addressing the operator's perception of smoothness. [Gomes, 1997] He first took Davis's idea of mapping available clutch torque in joint space and applied it to tip space. Though joint space mapping of clutch torque was a large step towards intuitively understanding what is happening, tip space is closer to what we perceive. When a compromise was made because the true desired torque could not be achieved, but only a component was satisfied, it was not clear how this translated to tip forces and movement with respect to the desired path. By working in tip space, we fully understand the consequence of an algorithm's compromise. In addition, Gomes simplified the target system to just a spring perpendicular to the path and did not take into consideration PTER's dynamics. Gomes experimented with blending the transition from clutch to clutch instead of immediately selecting new clutches when desired torque changed as Davis's algorithm did. The virtual trajectory was also expanded to include a straight line and/or a wall where movement was free on one side, but restricted on the other.

Gomes proceeded to attempt a new form of haptic control law. Instead of determining a desired force, he concentrated on limiting the 2 DOF device to 1 DOF most closely matching the desired return path or haptic boundary. When the tip had penetrated into the restricted region, a 45^{o} line was used as the desired path back to the unrestricted area. (See figure 2.6) He then locked the clutch that resulted in transferring PTER to a 1 DOF device most closely matching the return line. The next step was to use a combination of multiple modulated clutches to achieve the desired return line instead of locking one clutch. Again many variations of this algorithm were generated; ranging from further clutch blending to hybrid impedance/velocity based control. Gomes appeared to get descent trajectory following results, but hardware limitations became evident.

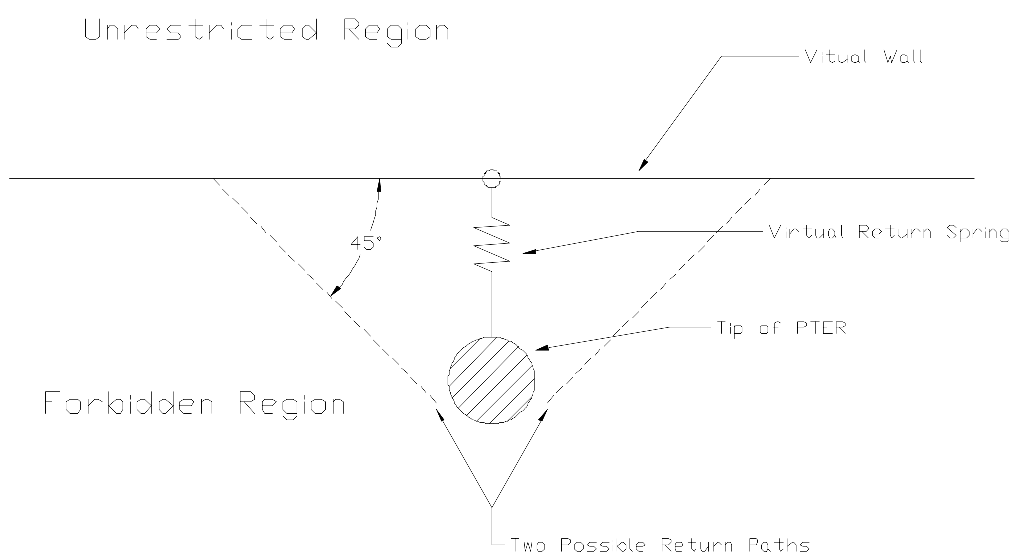

Figure 2.6: 45^o Return Paths to Virtual Wall

2.4.4 Current Author

Gomes's algorithm attempted to return the handle of PTER back to the unrestricted region along the 45^o path, but the control law disabled all of the actuators to allow free movement as soon as the operator crossed back over the virtual wall. From just viewing Figure 2.6, the return path appears to launch the operator out of the restricted region, immediately allowing unrestricted motion, causing the user to overshoot the virtual wall. In an attempt to minimize this, the algorithm was modified to choose a desired return path with an angle varying proportional to distance in the restricted region. Figure 2.7 illustrates this concept. As PTER's handle approaches a virtual wall, the angle of the return path decreases, allowing the operator to be directed back along the virtual boundary.

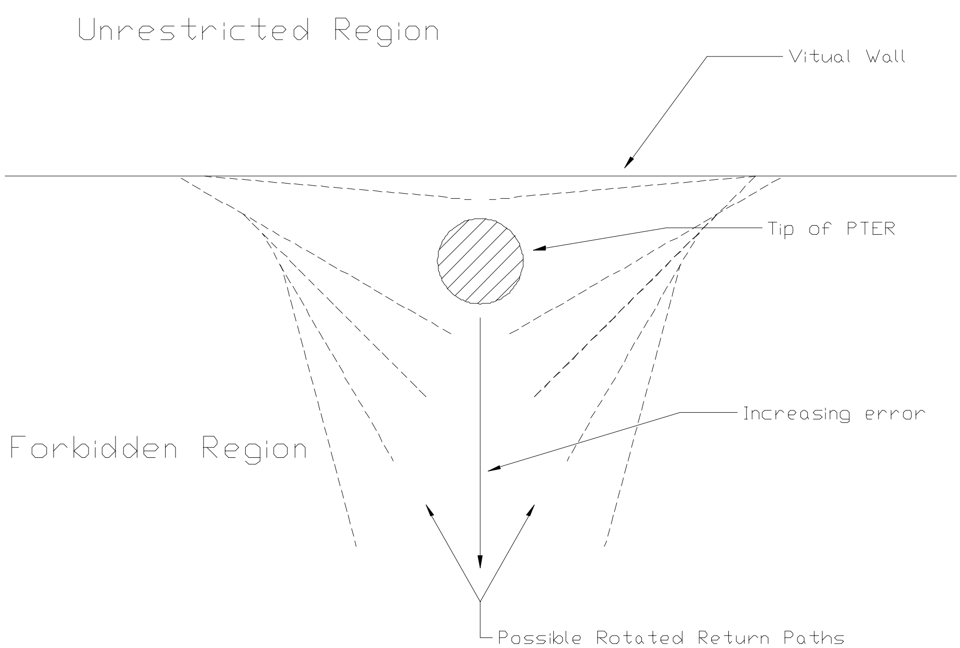

Figure 2.7: Varying Angle Return Path

In addition Gomes's algorithm was originally written to only simulate a horizontal wall. His code was modified, permitting simulation of a wall at any angle (horizontal, vertical, or slanted). Using this new code the virtual corridor in Figure 2.8 was replicated. The shaded area is where free motion is allowed while all remaining areas are restricted. Though no data was recorded on the performance of PTER in simulating this corridor, it is safe to say that PTER was successful in keeping the operator within the general area. It should be noted that performance was choppy and not highly accurate.

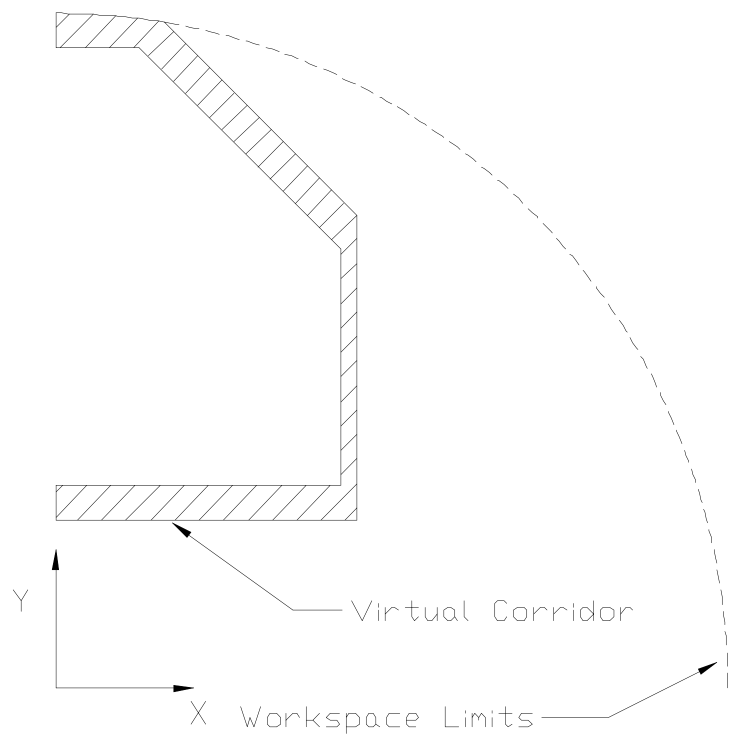

Figure 2.8: Virtual Corridor

2.5 Hardware Limitations

As expected, simulation results always proved better then implementation of the algorithms on PTER. It was also found that a large trade off existed between improved trajectory following and smooth performance. In order to successfully simulate virtual boundaries the clutch excitations were so high that they acted in an on-off fashion instead of being modulated. This contributed to jerky motion of the haptic device. The actuators were ideally modeled in the simulations and coding for PTER as having a linear relationship between supplied voltage and resulting torque with no dynamic response. In other words, as soon as the clutches received the voltage supply they immediately provided the requested torque in an open loop fashion. These are obviously unrealistic assumptions and though some work was done to identify the clutches' shortcomings, no effort was made to implement a controller that compensated. To make matters more complicated; friction clutches exhibit an undesirable nonlinear stick slip phenomenon as the coefficient of friction transitions from static to dynamic.

Both Mario and Will Stone attempted to map breakaway torque supplied by the clutches with respect to applied voltage, but this mapping was found to be non-linear. In addition, no two clutches acted the same. It should be noted that the clutches are rated to take 24 volts at roughly 2.4 amps continuously. Two of the power supplies were only capable of providing 1.5 amps of current. Thus, two of the power supplies were obviously under rated for powering the clutches. Mario attempted to capture a step response from one of the clutches and his results can be seen in figure 2.9. There appears to be both a pure time delay and an overdamped response. Additionally, the clutch never reached the desired torque.

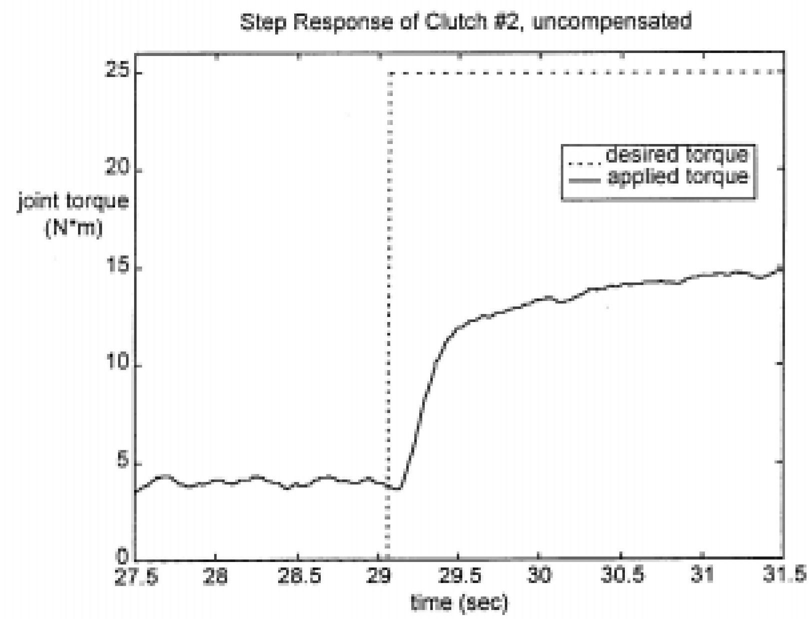

Figure 2.9: Clutch Step Response Results from Mario Gomes [Gomes, 1997]

From both this data and observation when using PTER, it can be concluded that the clutches are a weak link in the test bed. How can these clutches be modeled and/or modified for better performance? What can be done to implement closed loop feedback torque control? Should new clutches be substituted for the Dynacorp electromagnetic friction models? These are the issues that will be addressed through this Master's research. Other potential areas for improvement, such as sensor and hardware, will also be explored.